Electrical Thermal and Degradation Measurements of the LEAF e-plus 62-kWh Battery Pack

Marinelli, Mattia; Calearo, Lisa; Engelhardt, Jan; Rohde, Gunnar

Published in:
Proceedings of 2022 International Conference on Renewable Energies and Smart Technologies

Link to article, DOI:
10.1109/REST54687.2022.10023130

Publication date:
2023

Document Version
Peer reviewed version

Electrical Thermal and Degradation Measurements of the LEAF e-plus 62-kWh Battery Pack

Mattia Marinelli, Lisa Calearo, Jan Engelhardt
Department of Wind and Energy Systems
Technical University of Denmark (DTU)
Roskilde, Denmark
{matm; lica; janen}@dtu.dk

Gunnar Rohde
Danish Center for EnergyStorage
Danish Academy of Technical Science (ATV)
Copenhagen, Denmark
gr@atv.dk

***Abstract*—The paper provides a detailed description of the 62-kWh battery pack of the Nissan LEAF e-plus. Experimental measurements are collected and analyzed to identify electrical and thermal properties. The parameters identified are open circuit voltage, polarization resistance, diffusion resistances and capacitances. Measurements are carried out for different State-of-Charge and temperatures values. The current interruption method is used to identify the properties of the battery, since it is an effective way to analyze the whole battery pack without disassembling the vehicle. Afterwards, a cooldown analysis is described to identify thermal properties such as thermal capacitance and resistance. The paper is concluded with an early-stage assessment of the degradation of the battery pack after 1.5 years by using on-board readings of State-of-Health, temperature, and State-of-Charge. Stepwise changes in the State-of-Health are observed every 90 days superimposed to the expected degradation trend.**

Keywords—Battery pack; Battery degradation; Electric vehicle; Reverse Engineering; Thevenin equivalent; Testing.

I. Introduction

Batteries are widely recognized as key instruments in the green energy transition. Growing interest has been given to electric vehicles (EV), due to their large battery pack. Projects investigating how the battery in the EV can be used to support the electrical system and integrate more renewables have been flourishing in the last decade, particularly in Europe [1], [2]. Proper knowledge of the characteristics of EVs battery pack is needed, for example, to properly assess the internal State-of-Charge (*SoC*) [3], to characterize fast charging processes [4] or to evaluate profitability and degradation while providing grid services [5]. Thevenin equivalents are widely found in the literature when it comes to single cells tested in laboratory [6]. However, information and methods on commercial battery packs are limited, especially due to the lack of publicly available data. Even though the new European battery directive will require, in the future, manufacturers to provide access to battery management systems (BMS) [7]. To cover this gap, we have been performing tests and measurements on the widely known Nissan LEAF, focusing on the e-plus with 62-kWh battery pack. In a previous work, we performed similar investigations on the Nissan LEAF 40-kWh [8]. The key objectives are the following:

- To provide electrical and thermal measurements of the characteristics of the LEAF e-plus battery pack for different State-of-Charge (*SoC*) and temperatures.
- To assess State-of-Health (*SoH*) trend and discuss BMS algorithms based on 1.5 years of daily measurements.

The rest of the paper is structured as follows. Section II provides a general description of the battery pack under investigation, given information publicly available or retrieved through OBD-II. Section III explains the current interrupt method adopted to derive the electrical parameters of the battery pack and reports the related results. Section IV describes the method used to characterize the thermal properties of the battery pack. Section V focuses on the degradation process by analyzing on-board readings.

II. Battery Pack Overview

A. Battery pack publicly available information

The battery pack of the LEAF e-plus is manufactured by the company Envision AESC. According to information publicly available [9], there are 288 pouch cells using Lithium-Ion Nickel Manganese Cobalt Oxide (Li-NMC). The blend, though not confirmed, seems to be 532: 5 parts of Nickel, 3 parts of Manganese and 2 parts of Cobalt. The available information, including cells connections and weight are reported in TABLE I.

TABLE I. Battery pack publicly available information

Nameplate energy capacity	E_{label} (kWh)	62
Total number of cells	n_{cells}	288
Cells arrangement (series*parallel)	n_s*n_p	96*3
Net mass (only modules)	m (kg)	309
Gross mass including wiring, connections, and external casing	m_{gross} (kg)	440

B. Battery pack information derived via OBD-II

While public sources provide information on the number of cells as well as the nameplate capacity of the battery pack, it is not possible to retrieve specific information on the cell characteristics. By using an OBD-II reader and an application called Leaf Spy, it is possible to read the nominal battery capacity, which is equal to 176.4 Ah [10]. Considering that there are 3 cells in parallel, the individual cell capacity is equal to 58.8 Ah. The nominal battery voltage is derived by the nominal cell voltage, which is 3.65 V. Considering that 96 cells are in series, the overall nominal battery pack voltage is equal to 350.4 V. The corresponding nominal energy capacity is equal to 61.8 kWh. Values are summarized in TABLE II.

TABLE II. Battery pack information derived via OBD-II

Nominal Ah capacity	C_{nom} (Ah)	176.4
Nominal voltage	V_{nom} (V)	350.4
Nominal energy capacity	E_{nom} (kWh)	61.8

III. Electrical Characterization

A. Current interrupt method

The current interrupt method is a well-known approach used to determine electrical parameters of both cells and batteries [11]. It is important to highlight that the whole measurement campaign is done on the battery pack, thus all parameters reported in the paper refer to the whole battery.

Another important aspect to notice is that, since the battery pack is not disassembled from the vehicle, the battery can only be supplied via the standard charging ports: CHAdeMO or Type 2. This first measurement campaign derives open circuit voltage, polarization resistance, diffusion resistance and capacitance [12]. The purpose is to characterize the Thevenin equivalent circuit displayed in Fig. 1.

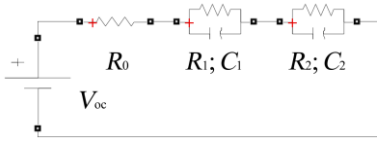

Fig. 1. Second order Thevenin equivalent with open circuit voltage, V_{oc}, polarization resistance R_0, and diffusion RC branches R_1, R_2, C_1 and C_2.

The tests are carried out by using an AC supply capable of providing up to 32 A on a single phase at 230 V. With this supply level, the on-board charger consumes 6.6 kW from the grid and injects 5.8 kW into the battery. Voltage and current are measured at the battery connection point, by using the EV on-board instrumentation. The charging level is sufficiently large to clearly identify voltage drops, but at the same time small enough to avoid influencing the temperature of the battery pack during the 10-hour tests. The charging sessions are carried out in sequences of 30 minutes of charge followed by 30 minutes of rest. They start with a *SoC* level below 10% and are completed once *SoC* is above 90%. Voltage, current and *SoC* values are read through the OBD-II port by using the Leaf Spy app. The EV is kept ON the whole time to ensure that the data acquisition system logs the values throughout the series of charging and resting sessions with 1-second resolution. It is unknown to the authors which type of voltage and current probes the LEAF internal instrumentation is equipped with, but it is reasonable to assume equipment with an accuracy of 1% on the current and 0.1% on the voltage [8]. The uncertainty on the *SoC* is assumed to be equal to 1%, as discussed in [14].

B. *Estimation of the electrical parameters*

Fig. 2 and Fig. 3 report two excerpts displaying voltage and current of a charging sequence with the 30-minute charging period, followed by a 30-minute resting period. It is highlighted how at the end of the 30-minute charging session, the current is interrupted to allow the assessment of the polarization resistance, R_0. The subsequent resting time of 30 minutes is used to derive the diffusion parameters, R_1, R_2, C_1, and C_2, along with V_{oc}. Values are assigned to the *SoC* level reached at the end of that specific charging sequence. By analyzing the first results (see Fig. 2), a single RC block is not sufficient to properly describe the behavior of the voltage. A second order equivalent circuit, including two RC blocks, namely long-term and short-term, is pursued instead. By using voltage and current readings, as illustrated in the examples reported in Fig. 2 and Fig. 3, it is possible to calculate the resistances as formulated in (1):

$$R_0 = \frac{V_{0-} - V_{0+}}{I_{0-} - I_{0+}};\ R_1 + R_2 = \frac{V_{0+} - V_1}{I_{0-} - I_1} \tag{1}$$

All quantities are a function of both *SoC* and temperature, thus their dependency is omitted. To derive the equivalent capacitive effect associated with the diffusion dynamics and splitting the parameters between short- and long-term time constant, the curve fitting tool provided by Matlab has been employed. By analyzing the resting period, a fitting with a single exponential is not adequate, therefore a double exponential fit, as reported in (2), is preferred:

$$\begin{cases} y(t) = V(t) - V_1 = (I_{0-} - I_1) \cdot (R_1 e^{-t/\tau_1} + R_2 e^{-t/\tau_2}) \\ \text{with } V(t) \in [V_{0+};\ V_1] \end{cases} \tag{2}$$

Each resting period is analyzed to derive the parameters that fit the specific session. The fit is considered adequate if the coefficient of determination is larger than 99%. Fig. 4 shows a graphical example of the fitting process. From the time constants, τ_1 and τ_2, it is possible to calculate C_1 and C_2, as reported in (3):

$$C_1 = {}^{\tau_1}/_{R_1};\ C_2 = {}^{\tau_2}/_{R_2} \tag{3}$$

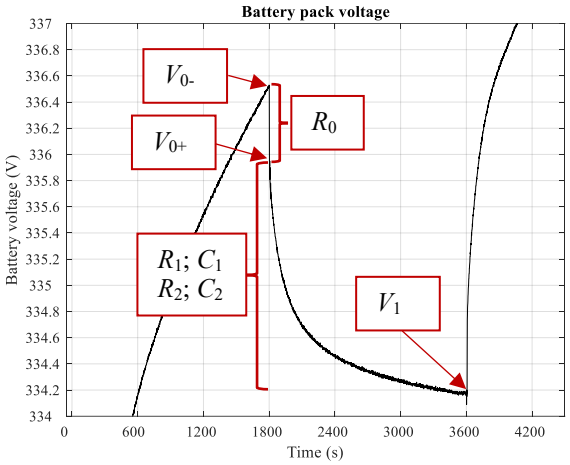

Fig. 2. Excerpt of the charging session subject to the current interrupt method with focus on the voltage during the first resting period at *SoC* of 11.7%.

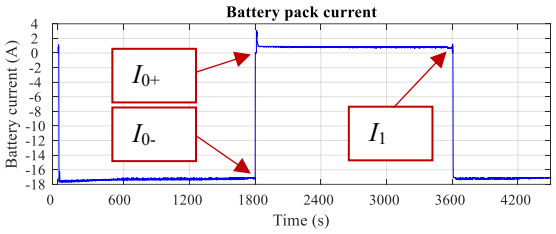

Fig. 3. Excerpt of the charging session subject to the current interrupt method with focus on the current behavior. While the EV is not charging, but still ON, there is a consumption of around 0.8 A to supply the auxiliary.

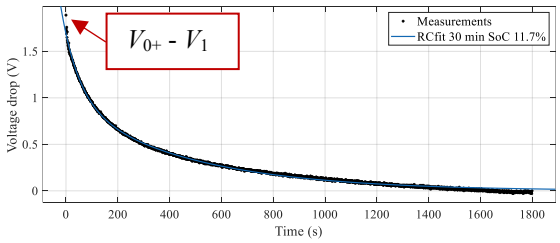

Fig. 4. Excerpt of the fitting method for the first 30-minute resting period: t=0 corresponds to the time where the current is interrupted.

As it can be seen from the end of the resting period in Fig. 4, the voltage has not completely stabilized yet due to the fact there is a small residual current, needed by the onboard electronics. However, considering the time constants of the long-term dynamics, it is acceptable to consider that the final voltage will not differ more than 5% from the value V_1. The open circuit voltage value V_{oc} is thus considered equal to V_1.

C. Overview of resistance and capacitance values

Since the charging power is low, the battery temperature was minimally influenced, therefore all values are obtained while the battery sensors measured 24±1 ºC. Resistance values for different *SoC* are shown in Fig. 5. *SoC* values refers to the whole battery capacity. The maximum voltage allowed on each cell is equal to 4.20 V, which implies a battery voltage of 403 V. The corresponding *SoC* is at 96-97% and the battery management system prevents further charging. The minimum voltage allowed for each cell is equal to 2.85 V, which implies a battery voltage of 274 V. Due to imbalances among the cells, during a deep discharge few cells may reach 2.85 V, while others are still above 3.00 V. Minimum battery voltages experienced during several tests were between 288 and 302 V with *SoC* between 0% and 2%.

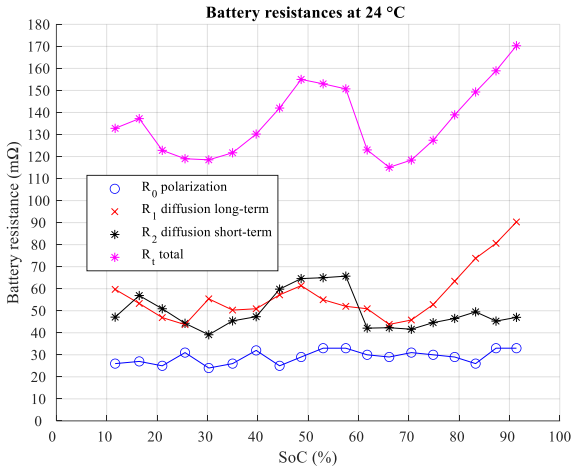

Fig. 5. Battery resistances R_0, R_1, R_2 and R_{tot} at 24±1 ºC.

Specifically, the polarization resistance R_0 shows a weak dependency on the *SoC*, while R_1 tends to increase for low and especially for high *SoC*. R_2 on the other hand presents local maxima in mid-range *SoC*, while low values are observed for high *SoC*. Detailed values are summarized in TABLE III. To give more general information on the battery, also the normalized total resistance is calculated in (4):

$$r_{\text{tot}} = (R_0 + R_1 + R_2) \cdot \frac{C_{\text{nom}}}{V_{\text{nom}}} \tag{4}$$

D. Temperature dependancy

While a battery temperature between 20 and 30 ºC is a common operating range during summer months in temperate climates, the derived electrical parameters may not be representative for winter months. To better characterize the Thevenin equivalent, selected measurements are repeated with a battery temperature at 4±1 ºC. Two representative *SoC* areas are chosen: 45-50% and 78-83%. The first area allows to capture the electrical behavior right before reaching the plateau in the 50-60% region, while the second area gives characterization before entering the high *SoC* values. The polarization resistance R_0 experiences a rather uniform increase with values 2.2-2.3 times larger compared to the ones at 24 ºC. The long-term diffusion resistances R_1 is marginally higher (1.1 times) in the 45-50% area, while it gets 1.4 times larger in the 78-83% area. On the other hand, the short-term diffusion resistances R_2 is marginally smaller (0.9 times) in the 45-50% area, while it gets 1.5 times larger in the 78-83% area. No noticeable variations of the open circuit voltage are observed. In general, an increase in the overall resistance can be observed, which is in line with the literature [11], [15]. Values are summarized in TABLE IV.

TABLE III. Battery pack electrical summary at 24±1 ºC.

State-of-Charge	Open circuit voltage	Polarization resistance	Diffusion resistance "long"	Diffusion resistance "short"	Time constant "long"	Time constant "short"	Diffusion capacitance "long"	Diffusion capacitance "short"	Total resistance (R_0+R_1+R_2)	Normalized total resistance
SoC (%)	V_{oc} (V)	R_0 (mΩ)	R_1 (mΩ)	R_2 (mΩ)	τ_1 (s)	τ_2 (s)	C_1 (kF)	C_2 (kF)	R_{tot} (mΩ)	r_{tot} (%)
6.7%	327.5									
11.7%	334.2	25.6	59.7	47.1	473	69	7.9	1.47	132.4	6.7%
16.5%	337.1	26.9	53.3	56.9	592	93	11.1	1.63	137.1	6.9%
21.0%	341.5	25.1	46.9	50.9	577	91	12.3	1.78	122.9	6.2%
25.6%	345.2	31.1	43.7	44.3	588	90	13.4	2.03	119.1	6.0%
30.3%	347.1	24.3	55.4	39.1	561	68	10.1	1.75	118.8	6.0%
35.0%	348.5	26.4	50.3	45.4	592	79	11.8	1.74	122.1	6.1%
39.7%	349.8	31.5	50.9	47.3	533	70	10.5	1.47	129.7	6.5%
44.4%	351.2	24.9	57.2	59.8	523	73	9.1	1.22	141.9	7.1%
48.6%	352.9	28.7	61.4	64.6	501	78	8.2	1.21	154.7	7.8%
53.0%	355.3	33.0	55.0	65.0	645	80	11.7	1.23	153.0	7.7%
57.5%	358.6	33.3	52.0	65.7	650	81	12.5	1.22	151.1	7.6%
61.7%	364.2	29.8	50.9	42.1	647	62	12.7	1.48	122.8	6.2%
66.1%	368.5	28.9	43.8	42.3	668	60	15.3	1.41	115.0	5.8%
70.5%	372.9	31.4	45.8	41.6	641	64	14.0	1.53	118.8	6.0%
74.9%	377.3	30.2	52.8	44.6	642	66	12.2	1.47	127.6	6.4%
79.1%	381.7	28.7	63.4	46.5	606	65	9.6	1.40	138.6	7.0%
83.3%	386.3	25.8	73.8	49.5	615	67	8.3	1.36	149.1	7.5%
87.3%	391.1	33.1	80.6	45.3	583	66	7.2	1.45	159.0	8.0%
91.4%	396.0	32.8	90.3	47.0	577	59	6.4	1.26	170.1	8.6%
94.5%	398.0									

TABLE IV. Battery pack electrical summary at 4±1 ºC.

SoC (%)	V_{oc} (V)	R_0 (mΩ)	R_1 (mΩ)	R_2 (mΩ)	τ_1 (s)	τ_2 (s)	C_1 (kF)	C_2 (kF)	R_{tot} (mΩ)	r_{tot} (%)
45.0%	351.5	60.9	65.8	54.3	514	71	7.8	1.31	181.0	9.1%
49.6%	354.0	64.3	62.6	60.3	535	79	8.5	1.30	187.2	9.4%
78.4%	379.4	62.5	84.5	74.0	582	84	6.9	1.13	221.0	11.1%
82.5%	384.0	57.6	105.7	75.3	549	80	5.2	1.07	238.5	12.0%

IV. Thermal Properties

A. Cooldown method

The LEAF has no active cooling system; therefore, the battery temperature is the result of the thermal balance between heat generated inside the cells and heat dissipated through the battery casing. When the car is not driven, no heat is generated inside the cells and the battery temperature equalizes with the outside. To determine the thermal properties of the battery pack, it has been decided to measure the evolution of the temperature once the battery was heated up after a long drive with fast charging. A week in winter characterized by an almost uniform temperature to minimize the influence of the environment was chosen. The resulting dynamics can be characterized by an exponential curve as presented in (5). The temperature difference, ΔT, depends on the initial temperature and the thermal time constant, τ_{TH}.

$$\Delta T(t) = \left(T_0^{\text{battery}} - T_0^{\text{outside}}\right) \cdot e^{-t/\tau_{TH}} \quad (5)$$

Using the same approach described in [8], we estimate the thermal resistance, R_{TH}, that can be used to characterize heat transfer via conduction. Given this thermal resistance, it is possible to derive the corresponding thermal capacitance, C_{TH}, as described in (6). Knowing the battery pack net mass, m, the specific heat capacity, c_p, can be calculated.

$$C_{TH} = {}^{\tau_{TH}}/_{R_{TH}} \; ; \; c_p = {}^{C_{TH}}/_{m} \quad (6)$$

B. Thermal characteristics

The initial battery temperatures were between 20.2 ºC and 22.6 ºC, while the outside temperature was 3 ºC. The outside temperature remained almost constant for two days with minor oscillations in the range of ±0.5 ºC. The delta between the battery temperatures and the outside is displayed in Fig. 6. Single exponential curves fitting the three sensors are also reported to highlight how the dynamics can be described by the equation presented in (5). From the three exponential fits it is possible to derive the time constants, which are equal to 15.6 h, 15.9 h and 17.5 h. The average value, 16.3 h, is taken as representative time constant, τ_{TH}, to characterize the battery as lumped thermal element. Considering the geometry of the pack, approximately 110 cm long, 90 cm wide and thickness between 10 and 20 cm, the resulting thermal resistance is estimated equal to 0.185 K/W. TABLE V summarizes the thermal properties of the battery pack. The resulting c_p is in line with values for Li-NMC batteries [16].

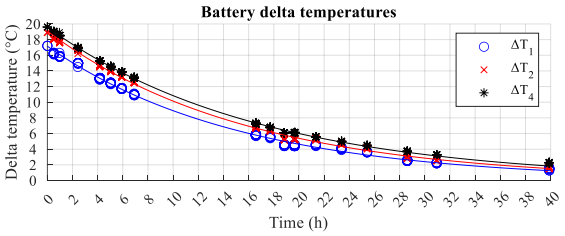

Fig. 6. Delta temperature for each sensor. Each circle represents a measured value, while the lines show the exponential fits.

TABLE V. Battery pack thermal summary

Thermal time constant (average)	τ_{TH} (h)	16.3
Thermal resistance	R_{TH} (K/W)	0.185
Thermal capacitance	C_{TH} (kJ/K)	317
Specific heat capacity	c_p (kJ/(K·kg))	1.03

V. Degradation Assessment

A. State-of-Health readings

An assessment on the battery degradation in the first 1.5 years is here discussed. The assessment is based on daily readings obtained by logging data when the EV is ON. Measurements have been taken twice per day, one in the morning before the EV is used for driving (or charging) and one in the evening. The first value is equal to 99.7% and was taken on the 2nd of December 2020, when the EV was delivered to the owner, living in Denmark. It is unknown to the authors how much in advance the battery pack was assembled. However, considering that it was manufactured in Smyrna (USA), and then shipped to Sunderland (UK) to be assembled with the rest of car, a lead time of 1 month is reasonable. As it will become clear in the next steps, the 27th of October is chosen as first day and a *SoH* equal to 100% is assigned.

Fig. 7 reports the quantity named State-of-Health in the Leaf Spy manual [10]. Two main trends can be observed. The first one influenced by the ambient, and subsequently battery, temperature: *SoH* tends to decrease more quickly over warmer months (May-September, which means days 185 to 340), while the decline is less steep elsewhere. The second one determined by recurring updates of the capacity estimation algorithm, taking place every 90 days.

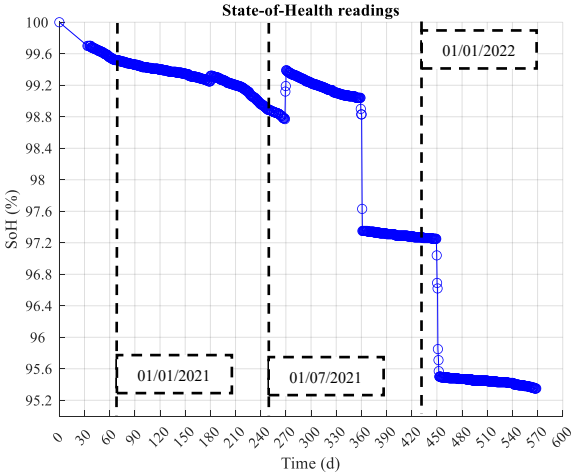

Fig. 7. *SoH* readings: each circle is a measured value. Large changes can be observed approximately every 90 days.

TABLE VI reports the dates when the *SoH* is subject to major changes: it is clear how the first steps happened after 6 and 9 months with increases, possibly due a periodic reassessment of the capacity estimation algorithm. Conversely, at month 12 and month 15, two reductions occur. It implies that this quantity, referred to as *SoH*, represents a figure of merit that accounts for degradation and capacity updates based on usage history and environmental conditions. To rule out the possibility of other factors such as high *SoC* periods, temperature, and heavy usage, influencing this *SoH* trend, other key quantities are discussed.

B. Battery and EV key indicators

Fig. 8 displays the battery temperature with the same time granularity used for the *SoH* values (i.e., two values per day). The EV is rarely used for long journeys (i.e., more than 300 km/day) and experienced few fast-charging sessions. Despite the lack of active cooling, the battery temperature does not deviate significantly from the ambient temperature and a

seasonal pattern can be observed. Over the 1.5-year period analyzed, the average battery temperature stands at 12 ºC against an average ambient temperature of 8 ºC. The charging processes are avoiding high *SoC* for long periods and are mostly based on slow charging [17]. An average *SoC* around 62% is observed throughout the same period.

Finally, the usage of the EV is rather regular as it can be seen from the distance values in TABLE VI, which means that cycling degradation is uniform across the period. The 90-day periods are grouped in each row and mean values for *SoC,* and battery temperature are reported along with the initial and final *SoH* for the period. The driven distance is also indicated to estimate the equivalent cycles: considering an average driving efficiency of 6 km/kWh, the battery experienced approximately 60 full equivalent cycles, which implies that cycling degradation is not the dominant degradation mechanism [5]. Calendar aging on the other hand dominates the process and it is worth remembering that it is mainly driven by *SoC* and temperature values, besides the passing of time [18]. Therefore, it tends to accelerate over warmer months while it reduces over colder months.

TABLE VI. Battery pack key indicators.

Periods	*SoH*	Delta *SoH*	Mean *SoC*	Mean Temp. (ºC)	Driven Distance (km)
27/10/2020 25/01/2021	100.00% 99.46%	-0.54%	49%	9.2	2631
25/01/2021 25/04/2021	99.46% 99.25%	-0.21%	59%	7.4	3036
25/04/2021 23/07/2021	99.32% 98.77%	-0.55%	58%	19.5	4647
24/07/2021 21/10/2021	99.39% 99.04%	-0.35%	65%	19.0	3968
23/10/2021 19/01/2022	97.35% 97.25%	-0.10%	61%	8.5	3356
23/01/2022 21/04/2022	95.50% 95.42%	-0.08%	62%	7.7	3140
22/04/2022 18/05/2022 (ongoing)	95.40% 95.35%	-0.05%	68%	15.8	1504

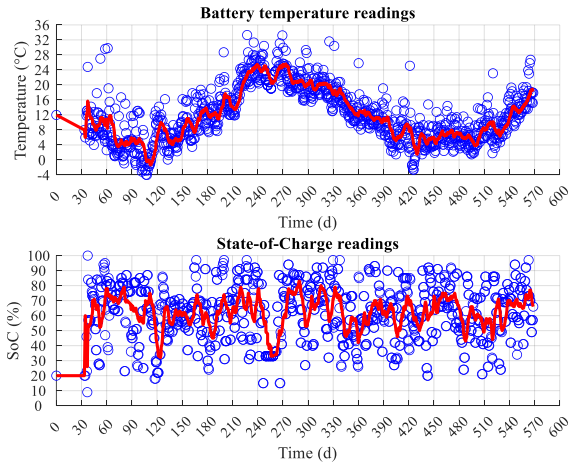

Fig. 8. Battery temperature and *SoC* readings: each circle is a measured value. The red lines represent rolling week averages.

VI. Conclusions and Future Work

An electrical, thermal and degradation assessment of the LEAF e-plus battery pack was presented. Electrical and thermal parameters are derived to describe the battery pack through Thevenin equivalents. The assessment degradation highlighted the energy irreversibly lost and the one limited due to seasonal patterns. The methodology adopted can be utilized to characterize other electric vehicles battery packs and extend the knowledge on battery packs, particularly to better characterize degradation mechanisms. Future work will include building and validating a dynamic model to investigate the performance of the vehicle for both driving and providing grid services.

Acknowledgments

The work has been partly supported by the research project ACDC (EUDP grant: 64019-0541). www.acdc-bornholm.eu

References

[1] M. Marinelli et al., "Electric Vehicles Demonstration Projects - An Overview Across Europe," 2020 55th International Universities Power Engineering Conference (UPEC), 2020.

[2] L. Calearo, M. Marinelli, C. Ziras, "A review of data sources for electric vehicle integration studies," Renewable and Sustainable Energy Reviews, vol. 151, 2021.

[3] R. Xiong, J. Cao, Q. Yu, H. He and F. Sun, "Critical Review on the Battery State of Charge Estimation Methods for Electric Vehicles," in IEEE Access, vol. 6, 2018.

[4] J. Engelhardt, J.M. Zepter, T. Gabderakhmanova, G. Rohde, M. Marinelli, "Double-String Battery System with Reconfigurable Cell Topology Operated as a Fast Charging Station for Electric Vehicles," Energies, vol. 14, 2021.

[5] L. Calearo, M. Marinelli, "Profitability of Frequency Regulation by Electric Vehicles in Denmark and Japan, Considering Battery Degradation Costs," World Electric Vehicle Journal, Vol 11, 2020.

[6] S. Nejad, D.T. Gladwin, D.A. Stone, "A systematic review of lumped-parameter equivalent circuit models for real-time estimation of lithium-ion battery states," Journal of Power Sources, vol. 316, 2016.

[7] EU Commission, "EU battery directive". Online available: https://eur-lex.europa.eu/legal-content/EN/TXT/?uri=CELEX%3A52020PC0798

[8] L. Calearo, A. Thingvad, C. Ziras, M. Marinelli, "Methodological approach to model and validate EV battery packs electro-thermal-aging dynamics," Journal of energy storage – under review.

[9] M. Kane, "Here Is The Nissan LEAF e+ 62 kWh Battery," InsideEVs, Jan. 2019.

[10] J. Pollock, "LeafSpy help version 1.50," user manual, Feb. 2022.

[11] G. L. Plett, "Battery Managements Systems Volume 1," Artech House, 2015.

[12] M. Dubarry, B. Y. Liaw, "Development of a universal modeling tool for rechargeable lithium batteries," Journal of Power Sources, vol. 174, 2007.

[13] A. Thingvad, L. Calearo, P. B. Andersen, M. Marinelli, "Empirical Capacity Measurements of Electric Vehicles Subject to Battery Degradation from V2G Service," Vehicular Technology IEEE Transactions on, vol. 70, Aug. 2021.

[14] V. Pop, H.J. Bergveld, P.H.L. Notten, J.H.G. Op het Veld, P.P.L. Regtien, "Accuracy analysis of the State-of-Charge and remaining run-time determination for lithium-ion batteries," Measurement, vol. 42, 2009.

[15] M. Thingvad, L. Calearo, A. Thingvad, R. Viskinde, M. Marinelli, "Characterization of NMC Lithium-ion Battery Degradation for Improved Online State Estimation," 2020 55th International Universities Power Engineering Conference (UPEC), 2020.

[16] E. Hosseinzadeh, et al., "A systematic approach for electrochemical-thermal modelling of a large format lithium-ion battery for electric vehicle application," Journal of Power Sources, vol. 382, 2018.

[17] M. Marinelli, "Chronicles of a prosumer - living by the sun," Smart charging webinar, 21 Sep 2021.

[18] P. Keil, S. F. Schuster, J. Wilhelm, J. Travi, A. Hauser, R. C. Karl, A. Jossen, Calendar Aging of Lithium-Ion Batteries, Journal of The Electrochemical Society 163 (2016) A1872–A1880.